Contemporary Trends in the Synthetic Aspects, and Magnetic Properties of 3*d*-4*f* Heterometallic Cubane, Partial Dicubane, and Partial Tetracubane Core-type Coordination Compounds

Bilash Chandra Roy,[a] Dr. Tufan Singha Mahapatra*[a]

[a]*Department of Chemistry, Faculty of Science and Technology, ICFAI University Tripura, Agartala-799210, Tripura (W), India; E-mail: tufansmp@gmail.com*

Abstract:

Over the past two to three decades, the synthesis of multinuclear 3*d*-4*f* complexes have been received significant interest owing to their fascinating topological structures, and intriguing properties in several areas, such as catalysis, magnetic materials, luminescent materials, and biomaterials. Compartmental ligands like Schiff bases are useful candidates in the manufacture of 3*d*-4*f* heterometallic multinuclear complexes as different coordination sites available for different metals. 4*f* ions like Eu(III), Dy(III), Tb(III), and Ho(III) are hard and oxophilic and preferentially interact with the oxygen-rich parts of ligands, while 3*d* ions like Mn(II/III), Fe(II), Ni(II), Cu(II), and prefer nitrogen atoms for binding. Lanthanide (III) ions are regarded as potential building blocks for new types of magnetic materials due to its large magnetic anisotropy, which arises due to large spin-orbit coupling and crystal field in a distinctive ligand environment. In this book chapter, we reviewed the synthetic aspects, and magnetic properties of 3*d*–4*f* coordination compounds with cubane, partial dicubane, and partial tetracubane cores.

Keywords: *Schiff base, Cubane, Partial Dicubane, Partial Tetracubane, Magnetic properties*

1. Introduction:

The synthesis of 3*d*–4*f* mixed metal ion complexes has received enormous interest during the last three decades due to their fascinating structural topology and exciting magnetic properties for both potential and theoretical applications. [1, 2, 3, 4, 5] The first 3*d*-4*f* systems were discovered by Gatteschi et. al in 1985 and produced the first heterometallic Cu-Gd-Cu complex that showed ferromagnetic interactions. Some of the already reported 3*d*-4*f* systems with a variety of nuclearities are $[Cu^{II}_4Ln_6^{III}]$, $[Cu^{II}_4Ln^{III}]$, $[Cu^{II}_9Ln_2^{III}]$, $[Ni^{II}_8Ln^{III}_6]$, $[Ni^{II}_6Ln^{III}_3]$, $[Co^{II}_4Ln^{III}_2]$, $[Co^{II}_2Ln^{III}]$, $[Co^{II}_2Ln^{III}_4]$, $[Mn^{II}_2Ln_2^{III}]$, $[Fe^{III}_4Ln_2^{III}]$, etc. In addition to this, various 3*d*-4*f* systems have been discovered providing different structural topologies e.g. cage-like, cubane core-like, ring-like, and wheel-like structures. The formation of such a 3*d*-4*f* mixed metal complex is an extremely intricate process and it is regarded as an art. The selection of ligands is the most important aspect of the formation of intriguing structures. Multiple donor atoms should be present in ligands to bridge metal ions. 3*d* and 4*f* metal ions have precedence to associate with distinct donor atoms like nitrogen and oxygen, according to HSAB principle. For the synthesis of 3*d*-4*f* heterometallic complexes, two main approaches are widely used from the standpoint of ligands: (1) design the ligands that can hold multiple coordination sited for both 3*d* and 4*f* metal ions; (2) introduction of suitable co-ligands that can assist the self-assembly processes where both lanthanide ions and transition metal ions can be coordinated with donor atoms in presence of multidentate ligands. The two synthetic processes to prepare such 3*d*-4*f* complexes are referred to as "assisted self-assembly", and "designed assembly" respectively. These sorts of multinuclear 3*d*-4*f* coordinate ion clusters exhibit Single Molecule Magnets (SMM) behavior. The area of molecular magnetism has attracted some attention in recent years due to enormous progress in the synthesis followed by nanosized dodecanuclear [Mn_{12}] aggregate showing a bistable magnetic ground state (S=10 ground state) and magnetic hysteresis. [6, 7] Multinuclear complexes assembled by judiciously prepared ligands, 3*d*, and 4*f* metal ions are captivating candidates for magnetic molecular materials, with great potential in the information storage device, spintronics, quantum computers, luminescence, and magnetocaloric materials. [8, 9, 10, 11] Among the all-lanthanide ions Dy^{III}, Tb^{III}, Gd^{III}, Yb^{III}, and Ho^{III} ions are known to show large magnetic anisotropy originating from the unquenched spin-orbit coupling. The 4*f* metal ion-based compounds usually give decent performance as compared to 3*d* metal ion-based SMMs, this is due to the strong magnetic anisotropy of lanthanide ions. 4*f* metal ion-containing systems also exhibit weak magnetic coupling interactions when present in the ligand coordination sites and bridge with one or more donor atoms. To boost the strength of magnetic coupling interactions as well as suppression of quantum tunnelling of magnetization (QTM), significant synthetic approaches have been taken for the building of a new generation of 3*d*-4*f* coordination complexes. [12, 13, 14, 15, 16, 17, 18, 19, 20, 21, 22] The intriguing structure and wide range of uses of hybrid multinuclear complexes have prompted many researchers to seek out new and improved instances. Nonetheless, creating hetero-metallic compounds is a difficult undertaking. Chemists must devise synthetic techniques for combining various metal ions in a single unit while managing nuclearities, spin carrier topology, and dimensionality of the final compounds. Another difficult issue is to avoid the competition between different metal ions for the same or comparable coordination sites, which could lead to the creation of homo-nuclear complexes or combinations of distinct species. In this book chapter, we have discussed the synthetic strategies and interesting magnetic properties of heterometallic 3*d*-4*f* complexes with Cubane, Partial Dicubane, and Partial Tetracubane core type geometries.

2. Syntheses and structural aspects of compounds containing Cubane cores

Debashis Ray et.al has recently synthesized a family of octanuclear Ni_4Ln_4 complexes [$Ni_4Dy_4(HL\mathbf{1})_4(\mu_2\text{-}OH)_2(\mu_3\text{-}OH)_4(\mu\text{-}OOCCH_3)_8](NO_3)_2$ (Ln = Gd (**1**), Tb (**2**), Dy (**3**), Ho (**4**), and Yb (**5**)) cubane type cores by the reaction of phenol-based Schiff base ligand (H_2**L1**) 2-[{(2-hydroxypropyl)imino}methyl]-6-methoxyphenol with lanthanide(III) nitrate (Ln = Gd, Tb, Dy, Ho, and Yb), nickel(II) acetate and LiOH (Figure 1a). Single-crystal X-ray diffraction study of all the five complexes (**1**, **2**, **3**, **4**, **5**) revealed that they were isostructural, with a difference only in the number of water molecules (H_2O) present within the crystal structure. Complexes **1**, **3**, and **4** crystallized in the $P\bar{1}$ triclinic space group with Z = 1, whereas complex **2** and **5** crystallized in the *C*2/*m* monoclinic space group with Z = 2. The Ni_2Dy_2 cubic core belonging to the asymmetric unit of complex **3** was constructed by two Ni^{II} ions, two Dy^{III} ions, two HL^- from the ligand, three HO^- groups, and four AcO^- ions. Further, these two Ni_2Dy_2 cubic cores are connected by four AcO^- ions clips and two HO^- groups to develop a double cubane Ni_4Dy_4 structure. The tridentate pocket (ONO) of the ligand HL^- coordinated with one Ni^{II} center meridionally and an adjacent bidentate (OO) pocket of the ligand was used to trap the oxophilic Ln^{III} ion. [23] In the Ni_4Dy_4 complex, Dy_1^{III} and Dy_2^{III} prevailed in the distorted trigonal dodecahedral coordination environment, and Ni^{II} ions existed in a distorted octahedral coordination environment around the center. (Figure 1 b, c, d)

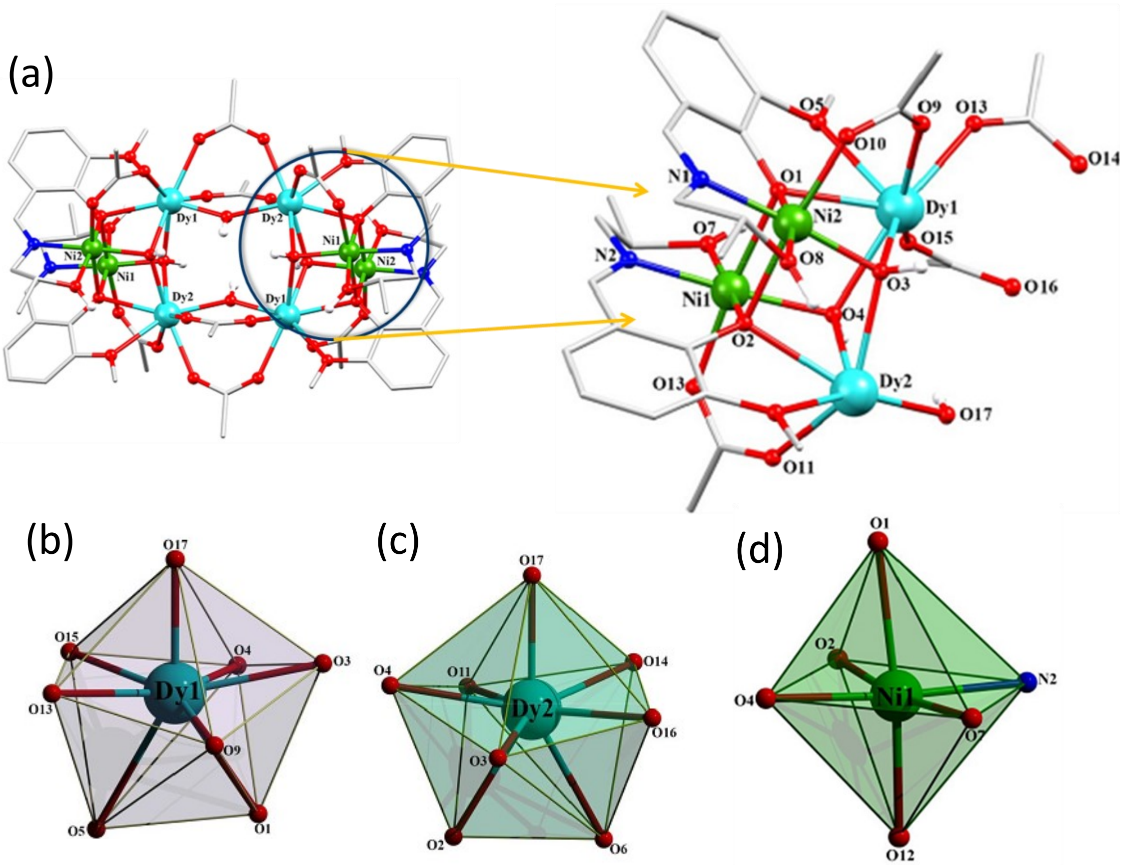

Figure 1: (a) POV-ray image of the asymmetric unit of Ni_4Ln_4 complexes. (b),(c),(d) In Ni_4Dy_4 complex Dy_1^{III} and Dy_2^{III} existed in a distorted trigonal dodecahedral coordination environment around the center and a Distorted octahedral coordination environment around the Ni^{II} center. Color code: O, red; N, blue; Dy^{III}, cyan; Ni^{II}, green. Reprinted with permission from reference 23. Copyright 2020 Wiley.

His, other work, reported a family of tetranuclear heterometallic Ni-Ln compounds $[Ni^{II}_2Ln^{III}_2(\mu_3\text{-}L\mathbf{2})_2(\mu_3\text{-}OH)_2(\mu\text{-}OAc)_3(AcO)(H_2O)_3]Cl_2\cdot 4H_2O$ (Ln = Gd, **6**; Tb, **7**; Dy, **8**; Ho, **9**) with cubane type cores by the reaction of 1-(2-hydroxy-3-methoxybenzylidene)semicarbazide (H**L2**) in presence of triethyl amine and sodium acetate. The Single crystal X-ray diffraction study of the complexes revealed that all the complexes formed tetranuclear [Ni_2Ln_2] compounds (**6-9**) having a $P2_1/n$ monoclinic space group with Z = 4 (Figure 2a). In this paper Ni_2Tb_2 complex (**7)** were chosen as representatives for detailed structural discussions. The tetranuclear $Ni_2Tb_2O_4$ hetero-cubane core was constructed by the two μ_3- PhO^- (O1 and O2) fragments of the ligand ($L2^-$) and two μ_3-HO^- (O3 and O4) groups which were generated from water molecules and three μ-O, O′-acetato (Figure 2b). The $\mu_{1,3}$-AcO^- bridges in three faces (two Ni···Tb and one Tb···Tb) of the cube supported the aggregation process. Nickel (II) ion present in all the structures showed distorted octahedral geometry in the NO_5 coordination environment. The Tb1and Tb2 present in the structure existed as coordination number 8, where Tb1 displayed distorted triangular dodecahedron geometry, but Tb2 exhibited distorted square antiprismatic geometry (Figure 2c,d,e). The eight coordination sites of Tb^{III} are fulfilled by the bidentate coordination (OO donor) from $L2^-$, two hydroxide and acetato bridges, and two terminal monodentate coordination from H_2O molecules for Tb2 center and one terminal monodentate H_2O and one AcO^- molecules to the Tb1 center. [24]

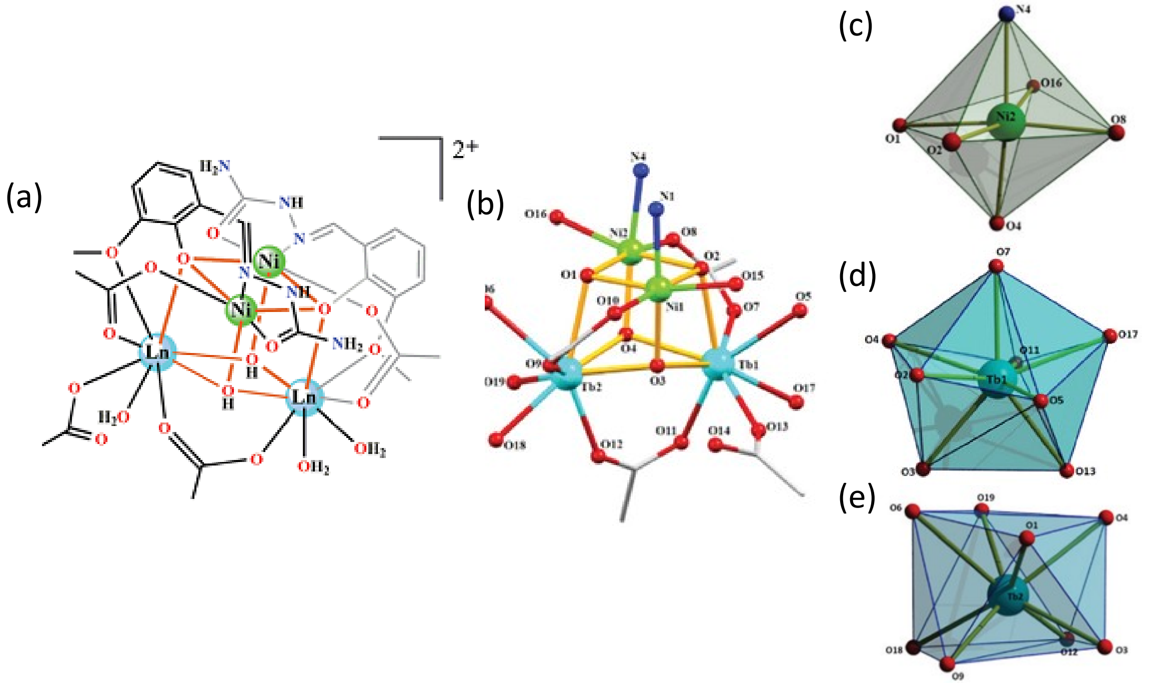

Figure 2: (a) Crystal structure of compounds **6-9**. (b) Cubane-like Core view of **7**. Color scheme: Tb cyan; Ni green; O red, N blue, C gray. (c, d, and e) Ni^{II} centers in distorted octahedral coordination environment, Distorted triangular dodecahedron around $Tb^{III}1$, and distorted square antiprism coordination geometry around $Tb^{III}2$, respectively. Reprinted with permission from reference 24. Copyright 2020 Royal Society of Chemistry.

A work carried out by Zhiliang Liu et.al has reported three novel heterometallic Ln_2Ni_2 clusters [$Ln_2Ni_2(\mu_3\text{-}OH)_2(OH)(OAc)_4(HL\mathbf{3})_2(MeOH)_3](ClO_4)\cdot 3MeOH$ [Ln = Dy (**10**), Tb (**11**), and Gd (**12**)] representing a new 3d-4f heterometallic motif with cubane type core. [25] These complexes were synthesized by the reaction of lanthanide (III) perchlorate (Ln = Dy (**10**), Tb (**11**), and Gd (**12**)), nickel (II) acetate, and 2-(benzothiazol-2-ylhydrazonomethyl)-6-methoxyphenol ligand (H_2**L3**) in presence of NaOH (Figure 3a). The Single-crystal X-ray diffraction studies of all the compounds (**10**, **11**, **12**) revealed that all compounds were isostructural, and the central core possesses [$Ln_2Ni_2O_4$] cubane core. All three complexes (**10**, **11**, **12**) crystallize in P*na*2_1 orthorhombic space group. Tb_2Ni_2 complex (**11**) was taken as a representative example. The tetranuclear metal centers in the Tb_2Ni_2 complex (**11**) were linked by two μ_3-phenoxido oxygen atoms and two μ_3-hydroxido groups from two $HL3^-$ ligands resulting in a cubic arrangement of the metal ions. The N, N, and O, O pockets present in the ligand coordinated with Tb^{III} and Ni^{II} metal ion in an anti-parallel fashion, it was further bridged with acetates in μ-η^1:η^1fashion to construct heterometallic cubane. The Tb1 and Tb2 center in the complex formed dodecahedral and bicapped trigonal prismatic geometry having an eight-coordinate number. On the other hand, the Ni^{II} ion present in the complex showed distorted octahedral geometry. The basal plane of the octahedron consisted of one bridging phenoxido (PhO^-) oxygen atom and two nitrogen atoms belonging to one HL**3**$^-$ ligand and the fourth coordination site was occupied by one oxygen atom from a bridging hydroxido group. The axial positions of the basal plane were occupied by two oxygen atoms, one was from the acetate group and another one was from the phenoxido (PhO^-) oxygen atom of a second HL**3**$^-$ ligand (Figure 3b).

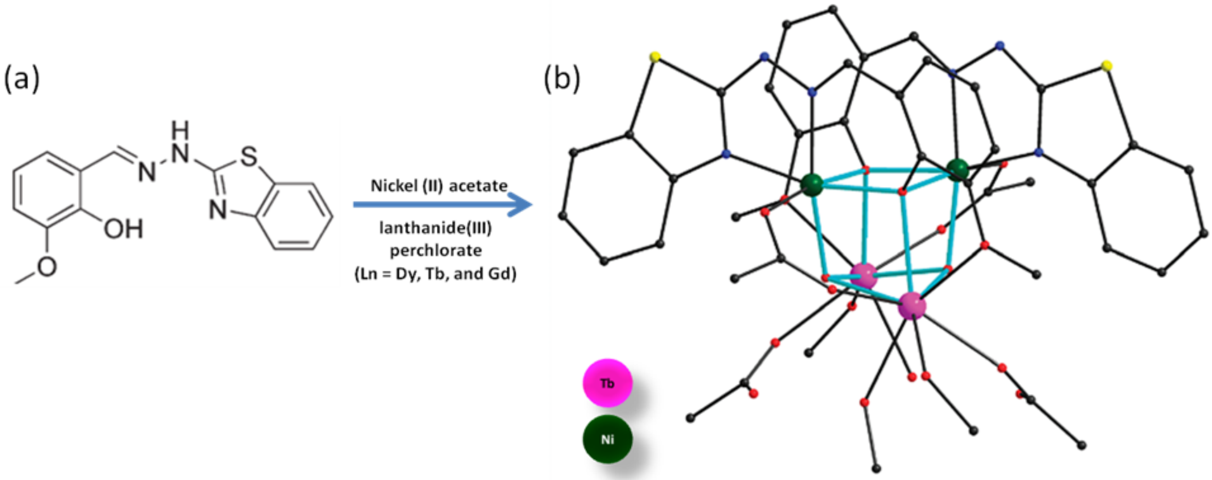

Figure 3: (a) Structure of Ligand H_2**L3** (b) Representation of the molecular structure of [$Tb_2Ni_2(\mu_3\text{-}OH)_2(OH)(OAc)_4(HL3)^{2-}(CH_3OH)_3]^+$ (**11**) with the [$Tb_2Ni_2O_4$] heterometallic cubane core. Hydrogen atoms are omitted for clarity. Color scheme: Tb pink, Ni green, O red, N blue, S yellow, C gray. Reprinted with permission from reference 25. Copyright 2011 American Chemical Society.

3. Syntheses and structural analyses of compounds containing Partial Dicubane cores

In recent years, Ray et.al. have synthesized a family of four Ni-Ln isostructural butterfly-shaped partial dicubane core complexes [$Ln_2Ni_2(L4)_2(\mu_3\text{-}OCH_3)_2(\mu_{1,3}\text{-}PhCO_2)_2(PhCO_2)_2(CH_3OH)_4]\cdot 2CH_3OH$ [where Ln=Gd (**13**), Tb (**14**), Dy (**15**) and Ho (**16**)]. [26] The four complexes have been synthesized by the reaction of 2-[{(2-hydroxy-benzyl)imino}methyl]-6-methoxyphenol Schiff base ligand (H_2**L4**) with $Ni(NO_3)_2\cdot 6H_2O$ and selected Ln^{III} nitrate salts [Ln= Gd (**13**), Tb (**14**), Dy (**15**) and Ho (**16**)] metal ions in presence of sodium benzoate as co-ligand and triethylamine as the base (Figure 4a). The Single-crystal

X-ray diffraction study established that all the four complexes (**13**, **14**, **15**, **16**) consisted of partial dicubane core (Figure 4b). The $Ni_2Ln_2O_6$ butterfly-shaped partial dicubane core of each complex was supported by two ($L4^{2-}$) ligand anions and two μ_3-OCH_3 groups. The Ni^{II} metal ion showed distorted octahedral geometry in all the complexes with coordination from two oxygen (O) atoms of ligand ($L4^{2-}$), two O of two μ_3-OCH_3 groups of MeOH, and one O from one benzoate group. Whereas Ln^{III} ion showed distorted trigonal dodecahedral geometry with eight coordination by three O atoms from two $L4^{2-}$ ligands, two O from the $-PhCO_2$ moiety, one O from the μ_3-OCH_3 group, and two O from MeOH solvent molecule (Figure 4c, d).

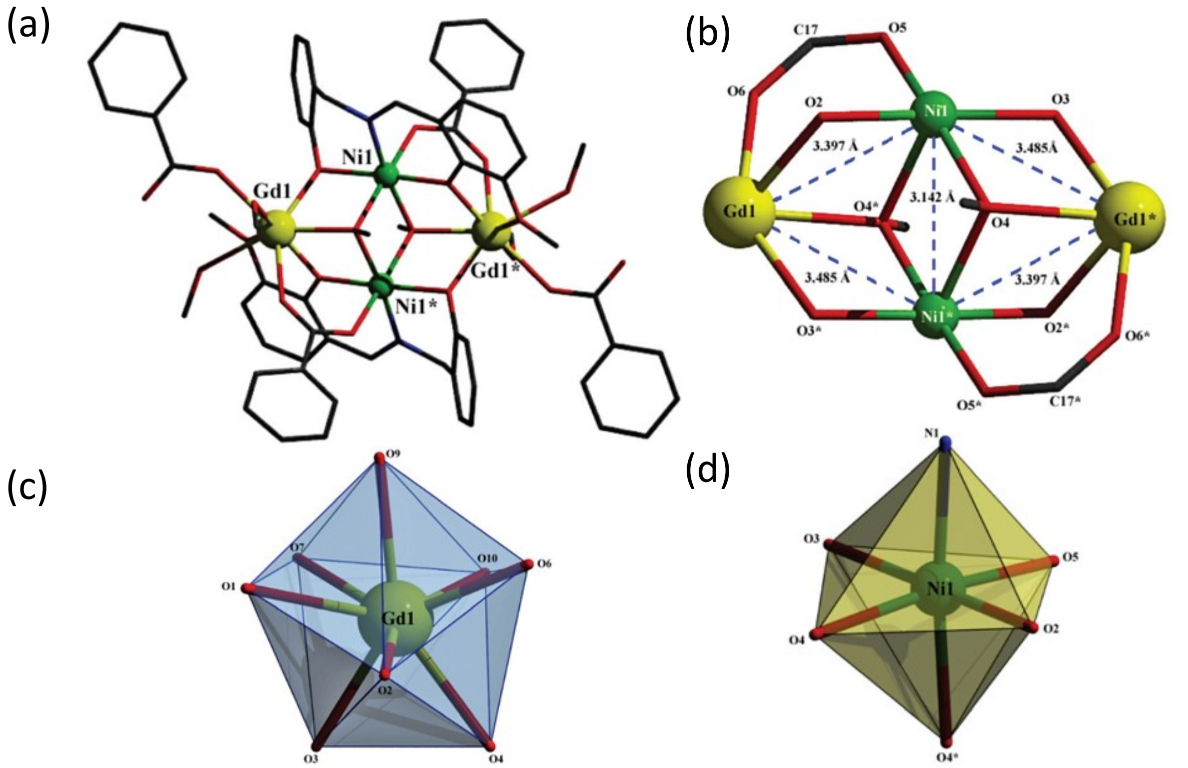

Figure 4: (a) Molecular structure view of complex **13**. H atoms and solvent molecules are removed for clarity. Colour code: C, grey; O, red; N, blue; Ni, green and Gd, yellow. (b) Distorted partial dicubane core of complex **13**. (c) Distorted trigonal dodecahedral geometry of Gd^{III} ions (left). (d) Distorted octahedral geometry of Ni^{II} metal ions (right). Reprinted with permission from reference 26. Copyright 2021 Royal Society of Chemistry.

4. Syntheses and structural aspects of compounds containing Partial Tetracubane cores

In another work, Debashis Ray et.al synthesized N_2O_4S donor atoms containing Schiff base ligand [2-((2-(2-(2-hydroxy-3-methoxybenzylideneamino)ethylthio)ethylimino)methyl)-6-methoxyphenol)] (H_2**L5**) and also explored its capability to give 3d-4f metal complexes (Figure 5a). The Schiff base ligand [2-((2-(2-(2-hydroxy-3-methoxybenzylideneamino)ethylthio)ethylimino)methyl)-6-methoxyphenol)] (H_2**L5**) was treated with $NiCl_2\cdot6H_2O$ and $Ln(NO_3)_3\cdot5H_2O$ in the presence of triethyl amine (Et_3N) in MeCN−MeOH (2:1) medium at room temperature resulted in three complexes of formula $[Ni_4Ln_2(L5)_2(\mu\text{-}Cl)_2(\mu_3\text{-}OH)_4(H_2O)_6]Cl_4\cdot2H_2O$, where Ln = Dy^{3+}(**17**), Tb^{3+}(**18**) and Ho^{3+}(**19**), which are having Partial Tetracubane cores (Figure 5b). [27] The authors also prepared $[Ni_4Ln_2(\mathbf{L5})_2(\mu\text{-}NCS)_2(\mu_3\text{-}OH)_4(NCS)_4(H_2O)_2]\cdot xMeOH.yH_2O$ (where Ln= Dy^{3+}(**20**), x =2, y =4; Tb^{3+}(**21**) and Ho^{3+}(**22**), x =0, y = 14.1) complexes **20**, **21** and **22** using the same Schiff base ligand $H_2\mathbf{L5}$ and $Ni(SCN)_2\cdot 4H_2O$, where SCN^- ions provided bridging and terminal coordination (Figure 5c). The Single crystal X-ray diffraction study revealed that all the six complexes acquire defective hexanuclear tetracubane cores having exchangeable bridging groups. Complex **17**, **18,** and **19** all are isostructural and all the complexes possess $P2_1/n$ monoclinic space group whereas Complex **20** and complex **21** showed $P\bar{1}$ triclinic space group but complex **22** crystallized in the $C2/c$ monoclinic space group. The crystal structure of complex **17**, which was taken as a representative among **17**, **18**, and **19**, has revealed that in pockets I each $L5^{2-}$ unit binds with two Ni^{II} centers whereas in pocket II asymmetric coordination of two 3d ions was observed. The pockets III and IV of the ligands were used to bind oxophilic Dy^{III} ions through the O, O donor part of the ligand. The hexanuclear centrosymmetric $Ni^{II}_4Ln^{III}_2$was formed by endogenous four μ-OPh groups and four exogenous μ_3-OH groups of four defective cubanes. On the other hand, the crystal structure of complex **20**, **21**, and **22** showed that all the three complexes are electro-neutral as the terminal water molecules were replaced by NCS^- ions which were bound to the Ni^{II} centers. Complex **20** and complex **21** crystallize in $P\bar{1}$ triclinic space group whereas complex **22** crystallizes in the $C2/c$ monoclinic space group. The single crystal X-ray diffraction study revealed that the core structure of complexes **20** and **22** was isostructural, difference only in solvent molecules present in the crystal structure. The μ_3-hydroxido groups along with μ-isothiocyanto groups were utilized to form the complex. In all the complexes (**17-22**) Ni ions formed distorted octahedral geometry but the Ln ions present in complexes (**17,18, 19**) formed distorted triangular dodecahedron geometry (Figure 5d), and in complexes (**20, 21, 22**) displayed distorted trigonal dodecahedral geometry (Figure 5e).

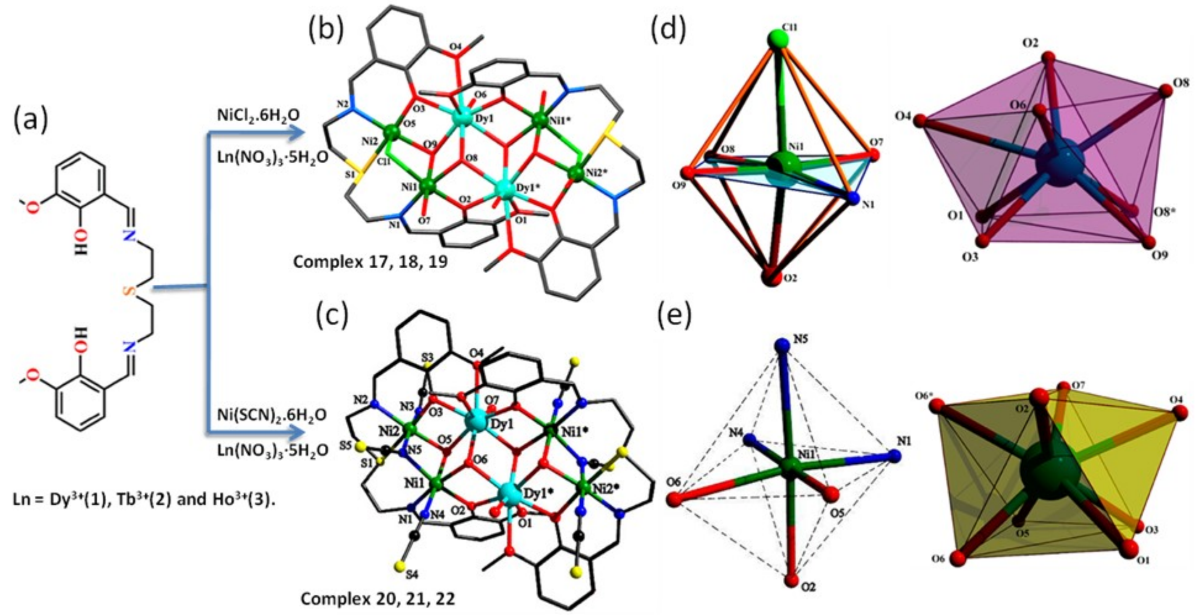

Figure 5: (a) Structure of $H_2\mathbf{L5}$. (b) Molecular structure of **17**, **18**, **and 19** with the partial atom numbering scheme**.** Hydrogen atoms, solvent molecules, and counter anions are omitted

for clarity. (c) Molecular structure of **20**, **21,** and **22**. (d) Distorted octahedral geometry around both the Ni(II) centers, and distorted triangular dodecahedron geometry around the Dy(III) centers in **17**, **18**, **and 19**. (e) Distorted octahedral geometry around the two Ni(II) centers, and Distorted trigonal dodecahedral geometry around the Dy(III) centers in **20**, **21,** and **22**. Reprinted with permission from reference 27. Copyright 2019 American Chemical Society.

Jinkui Tang et.al. have also reported a new family of heterometallic Ni_4M_2 hexanuclear clusters, $[Ni_4M_2(\mu_3\text{-}OH)_2(L6)_4(OAc)_2(NO_3)_2(H_2O)_2]\cdot kC_2H_5OH\cdot mCH_3OH\cdot nH_2O$ [M = Gd^{III} with k = 5 and n =1(**23**), Dy^{III} with k = 4 and n =2(**24**), and Y^{III} with k = 5 and m =1(**25**)] with partial tetracubane cores (Figure 6a). All three complexes were synthesized by the reaction of lanthanide(III) nitrate, and nickel(II) acetate with 2-(2-hydroxy-3-methoxybenzylideneamino)Schiff-base ligand (H_2**L6**) in the presence of triethylamine. All three complexes (1-3) have similar core structures with only a difference in the solvent of crystallization. The Single-crystal X-ray diffraction studies revealed that compounds **23** and **24** crystallize in the C2/*c* monoclinic space group whereas compound **25** was found in triclinic space group $P\bar{1}$. Each Ni_2DyO_4 subunit comprised of one Dy(III) ion and two Ni(II) ions arranged as a defective cubane with one missing vertex, through which the three metal ions are connected through three phenoxido groups and one hydroxido group. it was very interesting that the phenoxido groups adopt two types of coordination modes connecting the metallic ions. Two of three phenoxido groups adopted a doubly bridged mode, and each connected one Dy(III) ion and one Ni(II) ion, whereas the leftover one adopted a triply bridged mode binding with three Ni(II) ions, among which one Ni(II) ion was also a part of the adjoining cubane subunit (Figure 6b). The Ni(II) ions present in all three compounds are hexa-coordinated with the NO_5 environment; it can be viewed as distorted octahedral geometry and each Lanthanide ion is linked through phenoxido groups and the hydroxido group of the ligand towards the central Ni ions which provided Ni_2DyO_4 defective cubane core. [28]

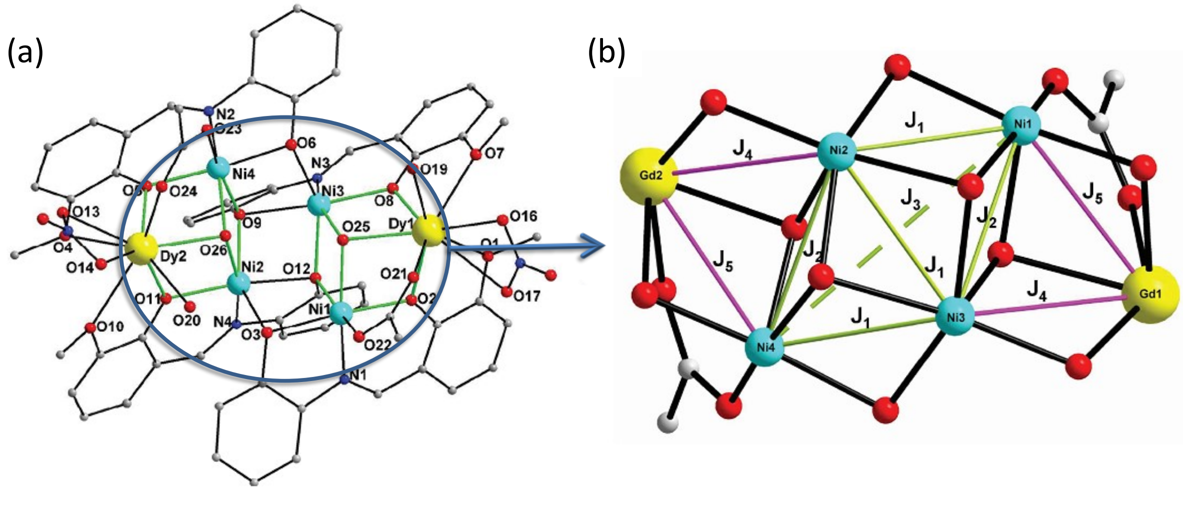

Figure 6: (a) Structure of the H_2L6 Ligand. (b) Molecular structure view of complex **24** highlighting the $[Ni_2DyO_4]$ heterometallic defective cubane subunits in bright-green lines.

Coordinated solvent molecules and H atoms are omitted for clarity. Reprinted with permission from reference 28. Copyright 2012 American Chemical Society.

5. Magnetic analyses of compounds containing cubane cores

The variable temperature magnetic study of the complexes $[Ni_4Dy_4(HL\mathbf{1})_4(\mu_2\text{-}OH)_2(\mu_3\text{-}OH)_4(\mu\text{-}OOCCH_3)_8](NO_3)_2$ (Ln = Gd (**1**), Tb (**2**), Dy (**3**), Ho (**4**), and Yb (**5**)) revealed ferromagnetic interaction between the existed metal ions. Further, frequency-dependent AC susceptibility measurements with no applied dc field displayed tails of an out-of-phase peak down to 2 K for Tb(III) (**2**) and Dy(III) (**3**) containing compounds (Figure 7b, c). These results indicated that among all the five complexes, most anisotropic lanthanide ions i.e Dy(III) and Tb(III) showed SMM behavior.

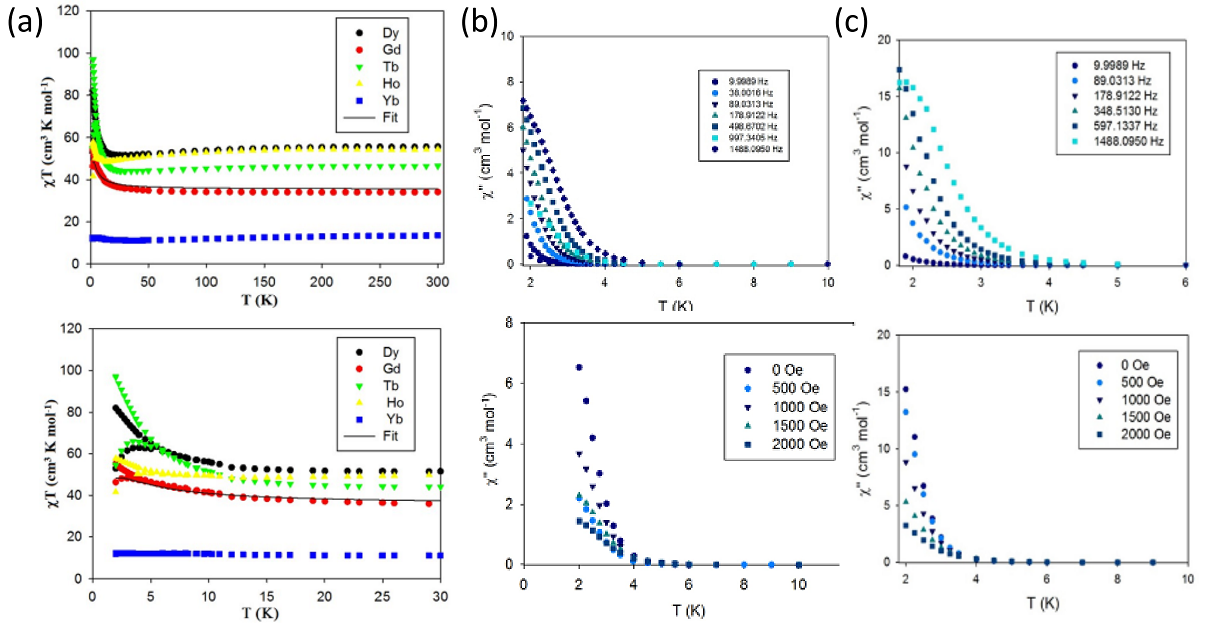

Figure 7: (a) Plots of χT vs. temperature for complexes **1–5** measured under a dc field of 3000 Oe (upper) and the low-temperature region with a dc field of 198 Oe for better meticulousness (down). The solid black line is a fit of the experimental data for complex **1**. (b) Out-of-phase ac magnetic susceptibility for **3** without applied dc field at the designated frequencies (upper) and the specified dc fields (down). (c) Out-of-phase ac magnetic susceptibility for **2** without applied dc field at the designated frequencies (upper) and the specified dc fields (down). Reprinted with permission from reference 23. Copyright 2020 Wiley.

Magnetic properties of tetranuclear heterometallic Ni-Ln compounds $[Ni^{II}_2Ln^{III}_2(\mu_3\text{-}L\mathbf{2})_2(\mu_3\text{-}OH)_2(\mu\text{-}OAc)_3(AcO)(H_2O)_3]Cl_2\cdot 4H_2O$ (Ln = Gd, **6**; Tb, **7**; Dy, **8**; Ho, **9**) have been studied at variable temperature to realize the role of magnetic anisotropy for the SMM behavior. All the complexes showed large ground state magnetic moment values and absence of out-of-phase ac susceptibility signals even in complex **8** which possesses Dy(III) ion due to the lack of axial anisotropy (Figure 8).

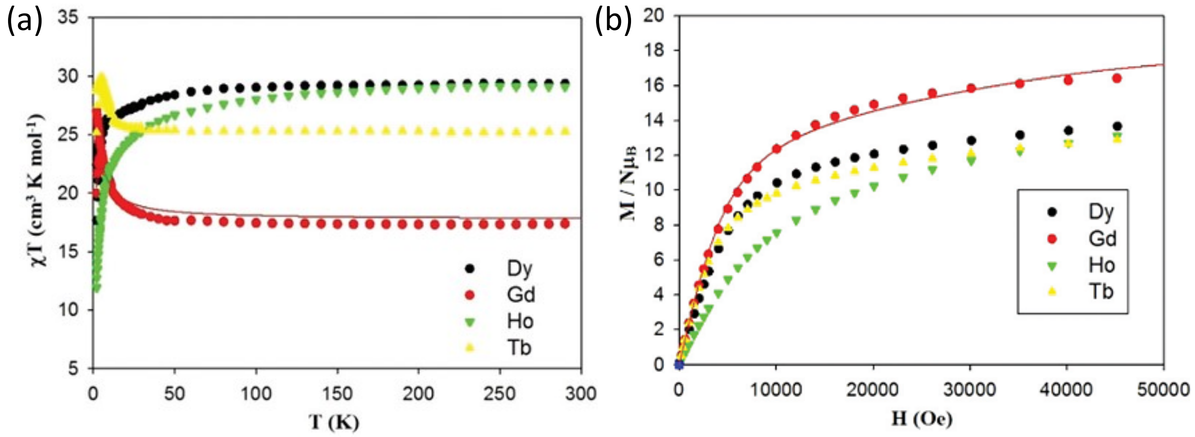

Figure 8: (a) χT products vs. T plot for the complexes **6–9**. The solid line is the best fit for the experimental data for complex **6** by utilizing PHI software. (b) Magnetization (M) vs. field (H) plots for complexes **6–9**. The solid line is the computed magnetization data for complex **6** using PHI software. Reprinted with permission from reference 24. Copyright 2020 Royal Society of Chemistry.

The magnetic study of $[Dy_2Ni_2(\mu_3\text{-}OH)_2(OH)(OAc)_4(HL\mathbf{3})_2(MeOH)_3](ClO_4)\cdot 3MeOH$ (**10**) complex revealed slow magnetic relaxation with frequency-dependent out-of-phase signal in AC susceptibility measurements (Figure 9). Whereas, in the DC field it was significantly slowed down which was generally showing up the presence of fast zero-field relaxation of magnetization. $[Gd_2Ni_2(\mu_3\text{-}OH)_2(OH)(OAc)_4(HL\mathbf{3})_2(MeOH)_3](ClO_4)\cdot 3MeOH$ (**12**) indicated ferromagnetic exchange interactions between Gd···Ni competing with Ni···Ni anti-ferromagnetic interactions.

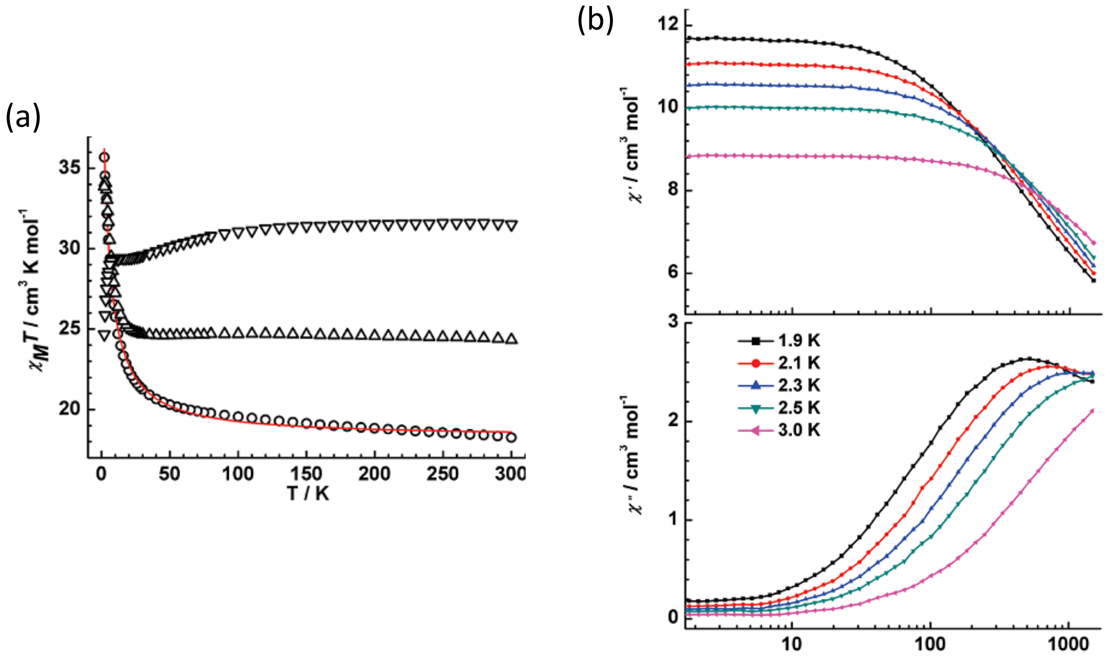

Figure 9: (a) Temperature dependence of the $\chi_M T$ products at 1 kOe for complexes **10**, **11**, and **12**. The red line is the simulation of the experimental data. (b) Frequency dependence of the in-phase (χ′) and out-of-phase (χ″) parts of the AC susceptibility for **10** with an applied

1200 Oe DC field. Reprinted with permission from reference 25. Copyright 2011 American Chemical Society.

6. Magnetic analyses of compounds containing Partial Dicubane cores

DC magnetic analysis study of the $[Ln_2Ni_2(L\mathbf{4})_2(\mu_3\text{-}OCH_3)_2(\mu_{1,3}\text{-}PhCO_2)_2(PhCO_2)_2(CH_3OH)_4]\cdot 2CH_3OH$; [where Ln = Gd (**13**), Tb (**14**), Dy (**15**) and Ho (**16**)], supported by DFT and CASSCF calculations showed dominating ferromagnetic exchange interactions between Ni–Ni ions ($J_{Ni\text{–}Ni}$ =7.16 cm^{-1}), and also between 3d–4f ions ($J_{Gd\text{–}Ni}$ = 0.715 cm^{-1}, $J_{Tb\text{–}Ni}$ =1.25 cm^{-1}, $J_{Dy\text{–}Ni}$ = 0.873 cm^{-1}, and $J_{Ho\text{–}Ni}$ = 1.42 cm^{-1}). An AC magnetic analysis study revealed that no slow relaxation was observed i.e., the complexes lack SMM characteristics (Figure 10).

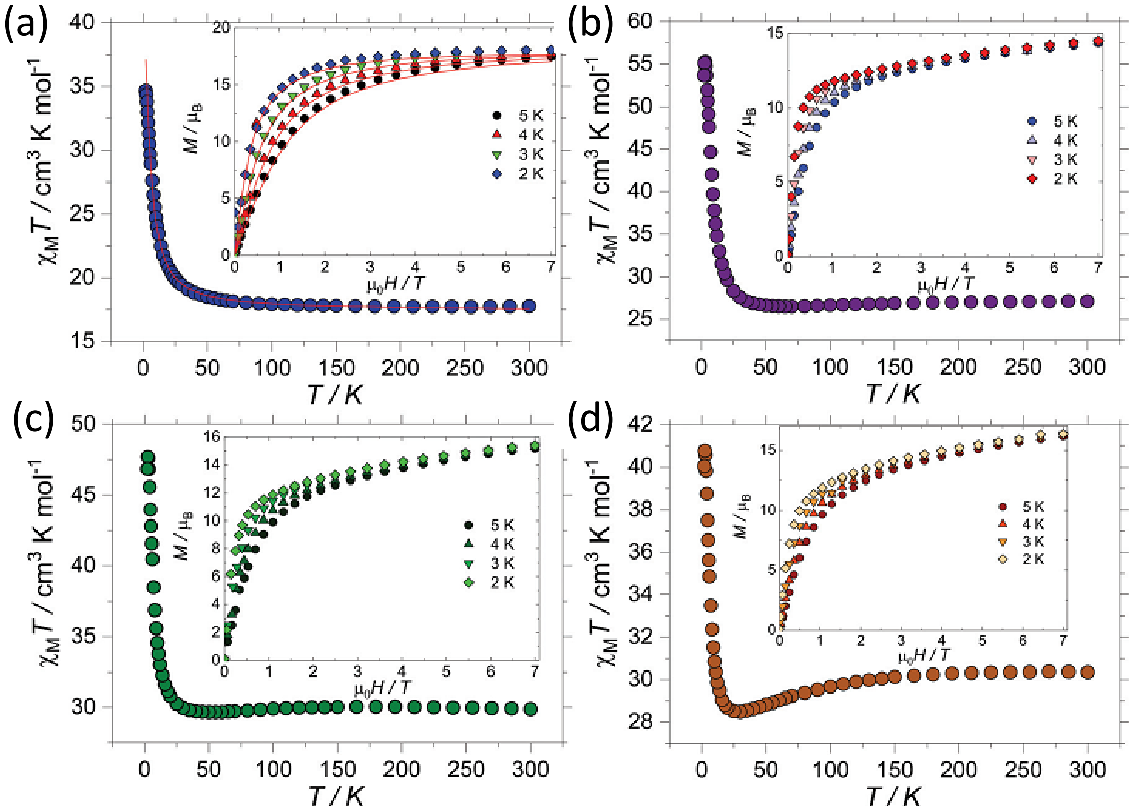

Figure 10: Temperature dependence $\chi_M T$ product and the isothermal magnetizations measured at = 2, 3, 4, and 5 K for (a) Ni_2Gd_2 (**13**); (b) Ni_2Tb_2 (**14**); (c) Ni_2Dy_2 (**15**); and (d) Ni_2Ho_2 (**16**). Reprinted with permission from reference 26. Copyright 2021 Royal Society of Chemistry.

7. Magnetic analyses of compounds containing Partial Tetracubane cores

AC susceptibility data of $[Ni_4Ln_2(L\mathbf{5})_2(\mu\text{-}NCS)_2(\mu_3\text{-}OH)_4(NCS)_4(H_2O)_2]\cdot xMeOH.yH_2O$ (where Ln= Dy^{3+}(**20**), x =2, y =4; Tb^{3+}(**21**) and Ho^{3+}(**22**), x =0, y = 14.1) complexes revealed an out-of-phase nonzero signal at zero static magnetic field, which confirmed the presence of slow magnetic relaxation for SMMs. Therefore, the temperature dependence AC susceptibility measurement was carried out (Figure 11). Both Ni_4Dy_2 (**17** and **20**) and Ni_4Tb_2

(**18** and **21**) complexes showed frequency-dependent maxima in the AC susceptibility (χ'') measurement. So, complexes **17**, **18** and **19**, **20** behave as SMMs at zero static field which was rare in other reports.

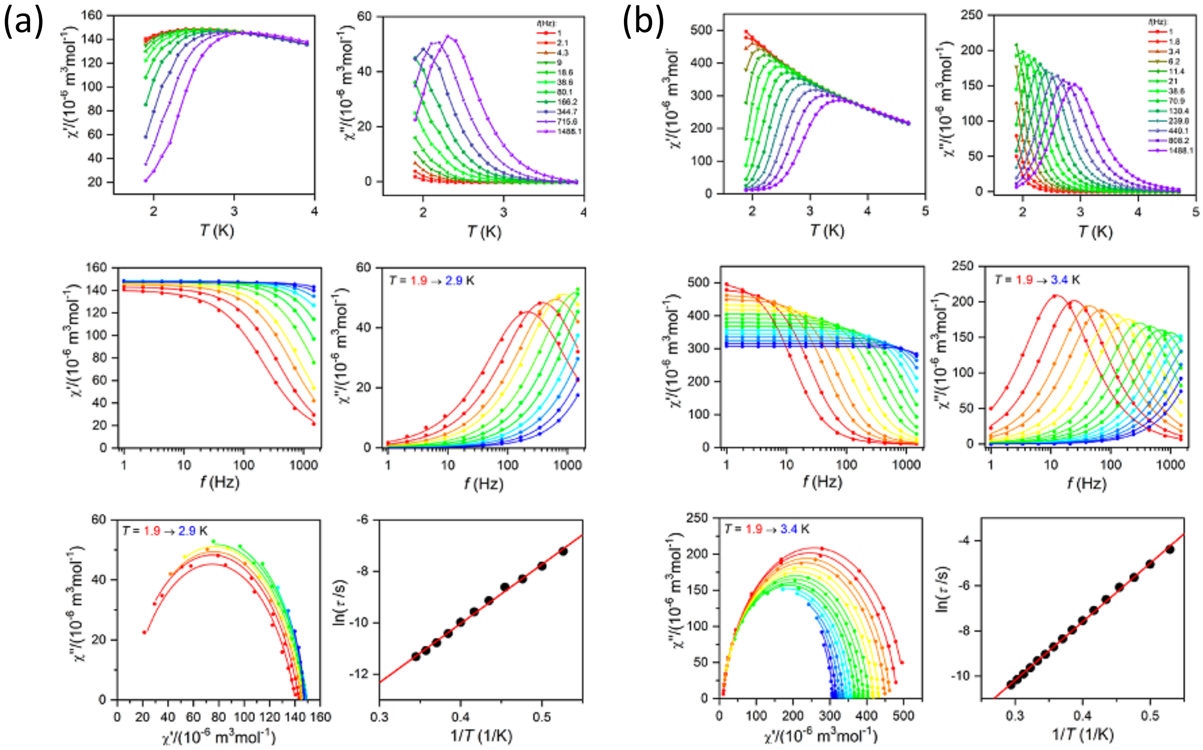

Figure 11: (a) AC susceptibility data for **17**. Top: in-phase χ' and out-of-phase χ'' molar susceptibilities at zero-magnetic field $B_{DC} = 0.0$ T; Middle: frequency dependence of in-phase χ' and out-of-phase χ'' molar susceptibilities; Bottom: Cole−Cole plot, on the right, the fit of resulting relaxation times τ with the Arrhenius law (red line). (b) Alternating current susceptibility data for **20**. Top: in-phase χ' and out-of-phase χ'' molar susceptibilities at zero-magnetic field $B_{DC} = 0.0$ T. Middle: frequency dependence of in-phase χ' and out-of-phase χ'' molar susceptibilities. Bottom: The Cole−Cole plot with solid lines; on the right, the fit of resulting relaxation times τ with the Arrhenius law (red line). Reprinted with permission from reference 27. Copyright 2019 American Chemical Society.

The magnetic study of $[Ni_4M_2(\mu_3\text{-}OH)_2 (L\mathbf{6})_4 (OAc)_2 (NO_3)_2 (H_2O)_2]\cdot kC_2H_5OH\cdot mCH_3OH\cdot nH_2O$; [M = Gd^{III} with k = 5 and n =1(**23**), Dy^{III} with k = 4 and n =2(**24**), and Y^{III} with k = 5 and m =1(**25**)] revealed that the Compound **23** (M = Gd) displayed a combination of antiferro- and ferromagnetic coupling pathways with no SMM behaviors. Whereas, in compound **24**, Dy(III) ions in the core lead to slow magnetic relaxation, which was further established by frequency-dependent out-of-phase ac signal (Figure 12). The magnetic properties of compound **25** indicated anti-ferromagnetic Ni···Ni exchange interactions competing with ferromagnetic exchange interactions, which are mediated by the Ni−O−Ni bridging angles.

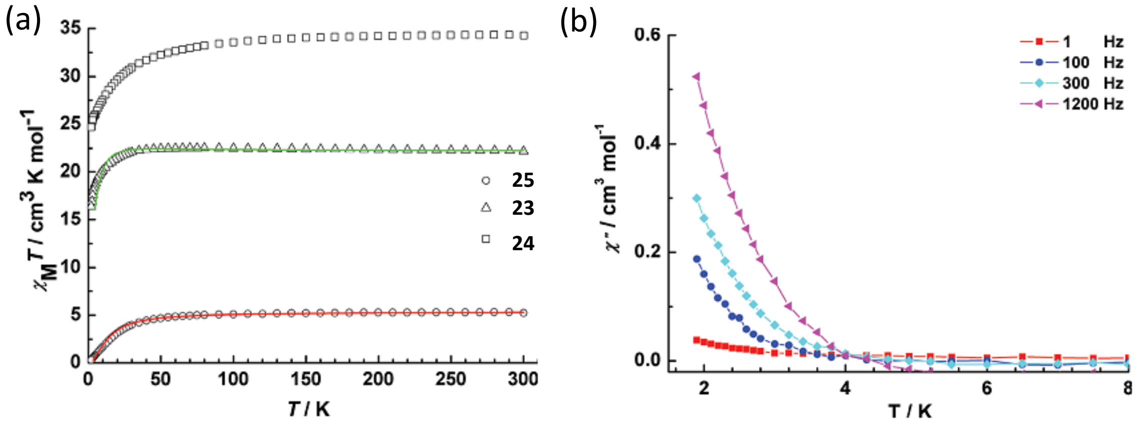

Figure 12: (a) Temperature dependence of the χ_MT products for compounds **23** (triangles), **24** (squares), and **25** (circles) at 1000 Oe. (b) Temperature dependences of out-of-phase (χ'') ac susceptibilities of **24** at different frequencies in a zero DC field and a 3Oe AC field. Reprinted with permission from reference 28. Copyright 2012 American Chemical Society.

CONCLUSION

In the past decade, the chemistry of heterometallic 3*d*-4*f* complexes has augmented rapidly due to the state-of-the-art technology available for characterizations such as single crystal X-ray diffraction and low-temperature SQUID measurements. The 3*d*–4*f* heterometallic complexes have also been considered to enhance the database of structural topology as well. Still, fairly a lot of effort endures for the development and understanding of the intricate magnetic properties of cubane core-based 3*d*–4*f* heterometallic complexes, which include the justifications of exchange interactions between 3*d* and 4*f* spin carriers and followed by theoretical computations to simulate the experiential magnetic behaviors. The slow relaxation of the magnetization required for the SMM behavior is regarded as the result of high anisotropic Ln^{III} ions for most 3d–4f SMMs. In summary, in this book chapter, we have discussed some recent literature reports of 3*d*–4*f* coordination compounds with cubane, partial dicubane, and partial tetracubane cores focusing on their synthetic aspects, and magnetic properties.

References:

[1] C. Aronica, G. Pilet, G. Chastanet, W. Wernsdorfer, J.-F. Jacquot, D. Luneau, A Nonanuclear Dysprosium(III)–Copper(II) Complex Exhibiting Single-Molecule Magnet Behavior with Very Slow Zero-Field Relaxation, Angewandte Chemie International Edition, 45 (2006) 4659-4662.

[2] N.F. Chilton, S.K. Langley, B. Moubaraki, K.S. Murray, Synthesis, structural and magnetic studies of an isostructural family of mixed 3d/4f tetranuclear ‘star’ clusters, Chemical Communications, 46 (2010) 7787-7789.

[3] Y.-Z. Zheng, M. Evangelisti, F. Tuna, R.E.P. Winpenny, Co–Ln Mixed-Metal Phosphonate Grids and Cages as Molecular Magnetic Refrigerants, Journal of the American Chemical Society, 134 (2012) 1057-1065.

[4] S. Hossain, S. Das, A. Chakraborty, F. Lloret, J. Cano, E. Pardo, V. Chandrasekhar, S-shaped decanuclear heterometallic [Ni8Ln2] complexes [Ln(iii) = Gd, Tb, Dy and Ho]: theoretical modeling of the magnetic properties of the gadolinium analogue, Dalton Transactions, 43 (2014) 10164-10174.

[5] M. Savva, K. Skordi, A.D. Fournet, A.E. Thuijs, G. Christou, S.P. Perlepes, C. Papatriantafyllopoulou, A.J. Tasiopoulos, Heterometallic MnIII4Ln2 (Ln = Dy, Gd, Tb) Cross-Shaped Clusters and Their Homometallic MnIII4MnII2 Analogues, Inorganic Chemistry, 56 (2017) 5657-5668.

[6] T. Lis, Preparation, structure, and magnetic properties of a dodecanuclear mixed-valence manganese carboxylate, Acta Crystallographica Section B, 36(1980), 2042-2046.

[7] R. Sessoli, H.L. Tsai, A.R. Schake, S. Wang, J.B. Vincent, K. Folting, D. Gatteschi, G. Christou, D.N. Hendrickson, High-spin molecules: [Mn12O12(O2CR)16(H2O)4], Journal of the American Chemical Society, 115 (1993) 1804-1816.

[8] M.N. Leuenberger, D. Loss, Quantum computing in molecular magnets, Nature, 410 (2001) 789-793.

[9] W. Huang, S. Huang, M. Zhang, Y. Chen, G.-L. Zhuang, Y. Li, M.-L. Tong, J. Yong, Y. Li, D. Wu, Multifunctional luminescent magnetic cryocooler in a Gd5Mn2 pyramidal complex, Chemical Communications, 54 (2018) 4104-4107.

[10] L. Bogani, W. Wernsdorfer, Molecular spintronics using single-molecule magnets, Nature Materials, 7 (2008) 179-186.

[11] R.J. Blagg, L. Ungur, F. Tuna, J. Speak, P. Comar, D. Collison, W. Wernsdorfer, E.J. McInnes, L.F. Chibotaru, R.E. Winpenny, Magnetic relaxation pathways in lanthanide single-molecule magnets, Nature chemistry, 5 (2013) 673-678.

[12] J. Long, F. Habib, P.-H. Lin, I. Korobkov, G. Enright, L. Ungur, W. Wernsdorfer, L.F. Chibotaru, M. Murugesu, Single-Molecule Magnet Behavior for an Antiferromagnetically Superexchange-Coupled Dinuclear Dysprosium(III) Complex, Journal of the American Chemical Society, 133 (2011) 5319-5328.

[13] C.-M. Liu, D. Zhang, X. Hao, D.-B. Zhu, Field-Induced Relaxation of Magnetization in a Three-Dimensional LnMOF with the Second Bridging Ligand Squarate, ACS Omega, 1 (2016) 286-292.

[14] Y.-N. Guo, G.-F. Xu, P. Gamez, L. Zhao, S.-Y. Lin, R. Deng, J. Tang, H.-J. Zhang, Two-Step Relaxation in a Linear Tetranuclear Dysprosium(III) Aggregate Showing Single-Molecule Magnet Behavior, Journal of the American Chemical Society, 132 (2010) 8538-8539.

[15] F.S. Guo, B.M. Day, Y.C. Chen, M.L. Tong, A. Mansikkamäki, R.A. Layfield, Magnetic hysteresis up to 80 kelvin in a dysprosium metallocene single-molecule magnet, Science (New York, N.Y.), 362 (2018) 1400-1403.

[16] F.-S. Guo, B.M. Day, Y.-C. Chen, M.-L. Tong, A. Mansikkamäki, R.A. Layfield, A Dysprosium Metallocene Single-Molecule Magnet Functioning at the Axial Limit, Angewandte Chemie International Edition, 56 (2017) 11445-11449.

[17] Y.N. Guo, G.F. Xu, W. Wernsdorfer, L. Ungur, Y. Guo, J. Tang, H.J. Zhang, L.F. Chibotaru, A.K. Powell, Strong axiality and Ising exchange interaction suppress zero-field tunneling of magnetization of an asymmetric Dy2 single-molecule magnet, J Am Chem Soc, 133 (2011) 11948-11951.

[18] R. Sessoli, A.K. Powell, Strategies towards single molecule magnets based on lanthanide ions, Coordination Chemistry Reviews, 253 (2009) 2328-2341.

[19] S.K. Langley, N.F. Chilton, L. Ungur, B. Moubaraki, L.F. Chibotaru, K.S. Murray, Heterometallic Tetranuclear [LnIII2CoIII2] Complexes Including Suppression of Quantum Tunneling of Magnetization in the [DyIII2CoIII2] Single Molecule Magnet, Inorganic Chemistry, 51 (2012) 11873-11881.

[20] C.-L. Yin, Z.-B. Hu, Q.-Q. Long, H.-S. Wang, J. Li, Y. Song, Z.-C. Zhang, Y.-Q. Zhang, Z.-Q. Pan, Single molecule magnet behaviors of Zn4Ln2 (Ln = DyIII, TbIII) complexes with multidentate organic ligands formed by absorption of CO2 in air through in situ reactions, Dalton Transactions, 48 (2019) 512-522.

[21] K.R. Vignesh, S.K. Langley, K.S. Murray, G. Rajaraman, Exploring the Influence of Diamagnetic Ions on the Mechanism of Magnetization Relaxation in {CoIII2LnIII2} (Ln = Dy, Tb, Ho) “Butterfly” Complexes, Inorganic Chemistry, 56 (2017) 2518-2532.

[22] J. Wu, L. Zhao, L. Zhang, X.-L. Li, M. Guo, J. Tang, Metallosupramolecular Coordination Complexes: The Design of Heterometallic 3d–4f Gridlike Structures, Inorganic Chemistry, 55 (2016) 5514-5519.

[23] M. Biswas, E.C. Sañudo, D. Ray, Octanuclear Ni4Ln4 Coordination Aggregates from Schiff Base Anion Supports and Connecting of Two Ni2Ln2 Cubes: Syntheses, Structures, and Magnetic Properties, Chemistry – An Asian Journal, 15 (2020) 2731-2741.

[24] M. Biswas, E.C. Sañudo, J. Cirera, D. Ray, Coordination control of a semicarbazide Schiff base ligand for spontaneous aggregation of a Ni2Ln2 cubane family: influence of ligand arms and carboxylate bridges on the organization of the magnetic core, New Journal of Chemistry, 44 (2020) 4812-4821.

[25] Y. Gao, L. Zhao, X. Xu, G.-F. Xu, Y.-N. Guo, J. Tang, Z. Liu, Heterometallic Cubanes: Syntheses, Structures, and Magnetic Properties of Lanthanide(III)−Nickel(II) Architectures, Inorganic Chemistry, 50 (2011) 1304-1308.

[26] A. Bhanja, R. Herchel, E. Moreno-Pineda, A. Khara, W. Wernsdorfer, D. Ray, Synthesis, characterization, magnetism and theoretical analysis of hetero-metallic [Ni2Ln2] partial di-cubane assemblies, Dalton Transactions, 50 (2021) 12517-12527.

[27] A. Bhanja, R. Herchel, Z. Trávníček, D. Ray, Two Types of Hexanuclear Partial Tetracubane [Ni4Ln2] (Ln = Dy, Tb, Ho) Complexes of Thioether-Based Schiff Base Ligands: Synthesis, Structure, and Comparison of Magnetic Properties, Inorganic Chemistry, 58 (2019) 12184-12198.

[28] H. Ke, L. Zhao, Y. Guo, J. Tang, Syntheses, Structures, and Magnetic Analyses of a Family of Heterometallic Hexanuclear [Ni4M2] (M = Gd, Dy, Y) Compounds: Observation

of Slow Magnetic Relaxation in the DyIII Derivative, Inorganic Chemistry, 51 (2012) 2699-2705.